Hindawi
Complexity
Volume 2023, Article ID 6636975, 18 pages
https://doi.org/10.1155/2023/6636975

Research Article

Dynamic Analysis of Isotropic Homogeneous Beams Using the Method of Initial Functions and Comparison with Classical Beam Theories and FEM

Jitendra Namdeo [1], **S. K. Dubey** [1] **and Lobzang Dorji** [2]

[1]*Department of Civil Engineering, Maulana Azad National Institute of Technology, Bhopal, India*
[2]*Department of Civil Engineering and Surveying, Jigme Namgyel Engineering College, Deothang, Bhutan*

Correspondence should be addressed to Lobzang Dorji; lobzangdorji.jnec@rub.edu.bt

Received 7 June 2023; Revised 23 October 2023; Accepted 21 November 2023; Published 9 December 2023

Academic Editor: Atila Bueno

The main aim of this study is the dynamic analysis of isotropic homogeneous beams using the method of initial functions (MIFs) and comparison with classical beam theories and FEM. Also, this research employs the state space methodology, with a special emphasis on isotropy, to analyse simply supported beam systems. A mathematical model for the dynamic response of beams is constructed using the method of initial functions. The novelty of this study lies in its approach to dynamic analysis, where isotropic homogeneous beams are explored without making assumptions, thus ensuring increased precision using the method of initial functions. Importantly, the approach remains free from restrictive assumptions and relies solely on mathematical formulations, yielding results superior to classical beam theories such as Euler–Bernoulli, Timoshenko, and Rayleigh beam theories. In this work, the application of MIFs of various orders (4th, 6th, 8th, and 10th) to calculate natural frequencies is explored, enabling a thorough examination of the beam's dynamic characteristics. In addition, parameters such as normal stresses, shear stresses, and deflections in different directions are considered to provide a comprehensive understanding of beam behaviour. To validate the findings, a detailed comparison with a finite element method (FEM) is conducted, achieving excellent agreement between the analytical results and FEM solutions. Furthermore, the influence of Poisson's ratio (μ) on natural frequencies is investigated by varying its value from 0.18 to 0.30. The research also explores the deviation of plane stress values of the beam section from those estimated using the FEM for the corresponding components.

1. Introduction

Every component of a structure vibrates freely. It implies that there are a fixed number of oscillations every second. Natural frequency is the term for the vibrations that occur naturally when a system seeks to oscillate freely. The system vibrates more intensely when forced to vibrate at its natural frequency (resonance). This bigger amplitude is undesirable for the structure's safety; hence, we must steer clear of this system's inherent frequency to get lesser vibrations. This paper aims to forecast the structure's intrinsic dynamic response, in terms of natural frequency and stresses and displacements, through a linear-free vibration analysis of a beam on which modern design techniques are founded.

The first person to address dynamic stresses in the beam structure was Timoshenko. Thomas and Abbas [1] represented a finite element model of a Timoshenko beam with nodal degrees of freedom. Three fixed-hinged Timoshenko beams excited by actual seismic motions were used by Kim and Cha [2] to test the validity of the formulation. Later, structures subjected to dynamic loading or seismic excitations are analysed using various methods, including time history analysis, response spectrum analysis, and frequency-domain spectral analysis. Singh and Ghafory-Ashtiany [3] developed a step-by-step modal time history integration method for dynamic analysis of earthquake-induced ground motions in nonclassically damped linear structures. Several parameters, such as spectral displacement, peak ground

acceleration, and absolute uniform duration, were used by Seyedi et al. [4] to characterize the earthquake ground motion. For the elastic response spectrum, Chopra [5] summarised the peak response to a specific component of ground motion of all probable linear single-degree-of-freedom (SDF) systems. In a simplified form, the background of the response spectrum method was presented by Gupta et al. [6], who worked on incremental response spectrum analysis (IRSA). At each piecewise linear incremental step, this method relies on a simple implementation of RSA. Solari and de Gaetano [7] demonstrated a collaborative calibration and progress of response spectrum analysis and frequency-domain analysis, resulting in findings that considerably agree, despite conceptual and operational differences.

Baghani et al. [8] studied the free vibration of large amplitude of tapered beams, and the governing equation is solved by the method of the variational iteration. Natural frequency for different mode shapes under different geometrical parameters is evaluated. Babaei et al. [9] analysed the functionally graded material beams for free vibrations. The support system of the beams is given over foundation of elastic nature. Governing equations of the beam are derived using higher-order displacement fields. Dimensionless amplitude parameters for mode shape one are derived to study the natural frequency of FGCP beams. Vatankhah et al. [10] worked on the exact controllability problem based on partial differential equations, and further numerical analysis was founded on the Hilbert uniqueness method and semigroup techniques and established the correctness of the results. Salarieh and Ghorashi [11], with the use of Hamilton's principle, analysed the cantilever beam for free vibration along with torsional and planar elastic bending deformations. Numerical analysis for different mode shapes establishes the Timoshenko beam theory and is being compared with other beam models. Jaworski and Dowell [12] investigated cantilevered beam flexural vibration with multiple cross-section steps. They compared experimental results to various theoretical methods, extending the analysis to different beam types. Alshorbagy et al. [13] discussed dynamic characteristics of functionally graded beams, focusing on material distribution, slenderness ratios, and boundary conditions' impact on beam dynamics through finite element analysis.

Shenas et al. [14], Malekzadeh and Heydarpour [15], and Malekzadeh et al. [16] examined the dynamic features of triangular plates, cylindrical shells, and three-dimensional conical shells of FGCP under a thermal environment. These works are constructed upon shear deformation theory along with the Chebyshev–Ritz technique and the principle of Hamilton. The elastic coefficients are used for deriving the eigenfrequency equations, and the differential quadrature method (DQM) is a numerical tool that is used to calculate geometric and frequency parameters. Pouresmaeeli et al. [17] first analysed double-orthotropic nanoplates which are simply supported and fixed from all edges. The effect of the external medium coupled from two sides, as well as the small-scale effect, is investigated on the basis of nonlocal theory. The dynamic properties of a viscoelastic nanoplate are also investigated using the nonlocal plate theory and the Kelvin–Voigt model. After establishing a governing equation with the help of numerical examples, the effects of external damping on frequency are studied. Non-dimensional frequency parameters for thick doubly curved FGCP are analysed by Pouresmaeeli and Fazelzadeh [18] with the use of Galerkin's method. The study employs various permutations of boundary conditions and geometrical constraints such as the thickness ratio and the aspect ratio to demonstrate the correctness of the proposed model. The natural frequency and other vibration characteristics are analysed by Mirzaei and Kiani [19] and Malekzadeh and Zarei [20] for composite plates with shell theory of first-order shear deformation (FSDT). The governing equation is solved by the eigenvalue problem with the help of the Ritz method, and by employing the differential quadrature method (DQM), numerical results unveil the importance of the volume fraction and the dispersion profile in dynamic analysis. Kiani [21] employed the Ritz formulation to derive the matrix illustration of the equations of motion related to the natural frequency of FGCP skew plates. Subsequently, parametric studies validate the volume fraction's influence on frequency parameters. Kiani [22] also investigated free vibration parameters of CNTRC plates through the layers of piezoelectric. Kiani et al. [23] analysed the natural frequency of FGCP of conical shapes with Donnell's theory and FSDT. To construct the shape function of the governing equation, the Gram–Schmidt process is used, and the numerical results are confirmed by a parametric investigation following convergence and comparison studies. Yildirim [24] delves into the vibration behaviour of functionally graded core sandwich insulation panels, meticulously considering material properties and grading's influence on natural frequencies. This study also introduces the complementary function method (CFM) as an efficient solution. Continuing the exploration of composite structures, Yildirim [25] investigates the free vibration characteristics of composite sandwich beams, emphasizing isotropic face sheets and an orthotropic core. Their use of the complementary function method in solving differential equations enhances precision. Shifting focus towards plate assemblies, Liu et al. [26] introduce a spectral dynamic stiffness (SDS) model. This versatile approach accommodates complex plate structures with different boundary conditions, incorporating beam stiffeners. It is validated with ANSYS, offering computational efficiency and robustness. Extending the applications of structural vibration analysis, Yildirim [27] harnesses artificial neural networks to estimate the properties of functionally graded beams. This innovative approach incorporates material properties, grading direction, and slenderness ratios, eliminating the need for solving differential equations or conducting time-consuming experiments. Meanwhile, Noori and Yildirim, [28] undertake a comprehensive investigation into the dynamic behaviour of pinned-pinned beams. Their study employs the finite element method with well-established software such as ANSYS and SAP2000, offering valuable results for both free and forced vibration responses. Stepping into the realm of material science, Al-Zahrani et al. [29]

explore the free vibration of plane stress strips composed of axial and bidirectional functionally graded materials using finite element modelling in ANSYS. Their research investigates the impact of material gradation and boundary conditions on natural frequencies, offering valuable insights for various structural applications. Marzavan and Nastasescu [30] advance the understanding of functionally graded materials (FGMs) in structural components. They introduce innovative concepts, such as the equivalent plate and multilayer plate, and validate their methodology through modal analysis and ANSYS simulations, providing accessible models for dynamic calculations of FGM structures. Tan et al. [31] also bring our attention to thin-walled box beams' free vibration characteristics, employing fine shear deformation theory and high-order beam theory for dynamic solutions. Their validation through finite element simulations in ANSYS highlights the role of various deformation modes in structural design, ultimately enhancing our understanding of these intricate structures.

The method of initial functions (MIFs) is a tool for analysing elasticity and structural mechanics. For rectangular regions, Vlasov invented the MIFs. The scientist derived the fundamental relations of the method for an isotropic continuum autonomously. This approach was extended by Das and Setlur [32] to two-dimensional elastodynamic problems. They developed a method for calculating stresses and deformations with the help of Sylvester's theorem and the Maclaurin series. The displacements and stresses on one layer of an elastic beam can be used to determine the displacements and stresses on adjacent layers. The MIF is exact in the results and very efficient in applications. The MIF is ubiquitous. It applies to all conditions and situations (static and dynamic). All kinds of structures (monolithic, composite, and layered) under various boundary conditions (simply supported, cantilever, and continuous) can be analysed through it. Multiple theories give approximate and exact solutions that can be extracted from the MIFs. Yet, its application is mostly seen in the field of static analysis of the structure. It has been widely used in varied work of static analysis of structures by Matrosov [33]. Very few researchers and scientists have used the method in structural dynamics. To calculate the natural frequency of a thick rectangular plate, Sundara et al. [34] employed the method of initial functions. Results corroborate the shear force and rotatory inertia effect in dynamic analysis. Sundara Raja Iyengar and Raman [35] took into account the free vibrations of arbitrary depth rectangular beams. It is an extension of the state-space method to the elastodynamic problem. Furthermore, they derived the MIF relation with the help of the eigenvalue problem and the Cayley–Hamilton theorem. Sundara Raja Iyengar et al. [36] examine the frequencies of rectangular plates' free vibrations with one or more fixed edges and varying thicknesses. Celep [37] and Celep [38] proposed a generalised version of the MIFs in cylindrical coordinates. They attained the free vibration parameters of a clamped circular plate. Goloskokov and Matrosov [39] analysed an anisotropic body for the three-dimensional elastodynamic problem. Based on relationships developed with MIFs, the bending of an orthotropic plate is considered. The load is assumed as a trigonometric series. These relationships are used to model the bending of orthotropic plates, with the load represented as a double trigonometric series.

Examples of sandwich plates with three layers and an aggregate with transverse isotropy are used to demonstrate how the method can be implemented using the MIF. When considering end effects, it is useful to describe results as series in Papkovich–Fadle eigenfunctions. Kovalenko et al. [40] and Kovalenko and Shulyakovskaya [41] developed a method for creating precise results for a half strip (rectangle) in the form of sequence in Papkovich–Fadle eigenfunctions based on the MIFs. To analyse reinforced concrete brick-filled composite beams, the MIF is used by Patel et al. [42]. For this, they devised problems based on equations of the MIFs. The stress block, which is employed in the limit state design of RC beams, is used to obtain the brick replacement zone. Petrosyan et al. [43] used the method of superposition to build a general solution for an orthotropic rectangle through the MIFs employing trigonometric series as initial functions. Patel et al. [44] analysed infilled beams with the usage of the MIFs and compared it with the results obtained from FEM analysis. They formulated the problems based on equations of MIFs. At first, the initial functions for the lowermost surface of the beam are determined with the help of the assumption of auxiliary function and boundary conditions. Furthermore, the stresses and deflections on the other layers of the beam can be determined. Patel et al. [45] investigated the result of changing Poisson's ratio on the beam's behaviour. It has been found that Poisson's ratio (μ) has little or no influence on stresses but has a considerable impact on displacements and strains. In the study conducted by Asutkar et al. [46], rubber aggregates are utilised in concrete to partially replace coarse aggregates and the impact on concrete properties is explored. Modified concrete is made of concrete that uses rubber aggregates in place of coarse aggregates and adjusts the replacement proportion. Using the method of starting functions, the stresses and displacements of beams are determined. Bending theory is compared to the MIFs for analytical results.

Matrosov et al. [47] provided a thorough assessment of the publications dedicated to the formation and advancement of the MIFs. They also emphasized its applicability to different engineering problems. In the realm of Fourier transforms, the MIF is considered. The results of eigenfunctions of the boundary value problem are given as improper Fourier integrals or series expansions. The MIF for micropolar media in plane strain conditions was also proposed by Matrosov [33]. In this study, he analysed a sample made of human bone, considering it a micropolar medium. His research is centred on the changes in the behaviour of "micropolar" stress-strain state components as the scale factor changes. MIFs can be used to formulate a solution in any definitive realm of the relevant coordinate system. In the present work, free vibration parameters under different support conditions are investigated with the help of mathematical formulations based on the MIFs. It is distinctive in contrast to the conventional high-order Taylor series approach, lumped mass method, and consistent mass

method; the present paper expands the state space method to two-dimensional elastodynamic problems. The preciseness of the results has been established with the help of results drawn from FEM. The effect of Poisson's ratios on the analysis is also investigated in this work. Patel et al. [48] also apply the method of initial functions (MIF) to analyse steel beam behaviour under various loadings. The MIF's hypothesis-free approach precisely resolves stress and strain, comparing results with bending theory, offering significant insights.

2. Formulation of Problem

The equations of dynamic equilibrium following the theory of elasticity for an axially symmetric condition according to Sundara and Raman [49] without body forces are

$$\frac{\partial \sigma_x}{\partial x} + \frac{\partial \tau_{yx}}{\partial y} = \rho \frac{\partial^2 u}{\partial t^2}, \qquad \frac{\partial \tau_{xy}}{\partial x} + \frac{\partial \sigma_y}{\partial y} = \rho \frac{\partial^2 v}{\partial t^2}. \tag{1}$$

For the state of plane stress, the stress displacement relations are as follows:

$$\sigma_x = \frac{E}{1-\mu^2}\left(\frac{\partial u}{\partial x} + \mu \frac{\partial v}{\partial y}\right), \quad \sigma_y = \frac{E}{1-\mu^2}\left(\frac{\partial v}{\partial y} + \mu \frac{\partial u}{\partial x}\right), \quad \tau_{xy} = G\left(\frac{\partial u}{\partial y} + \frac{\partial v}{\partial x}\right). \tag{2}$$

Let

$$U = Gu; V = Gv; X = \tau_{xy}; Y = \sigma_y, \qquad \frac{\partial}{\partial x} = \alpha; \frac{\partial}{\partial y} = \beta; \frac{\rho}{G}\frac{\partial^2}{\partial t^2} = \frac{1}{C_s{}^2}\frac{\partial^2}{\partial t^2} = \zeta^2. \tag{3}$$

Iyengar and Raman applied the state space methodology to two-dimensional elastodynamic problems. The following fundamental equation is obtained by removing σ_x between (1) and (2):

$$\beta \begin{bmatrix} U \\ V \\ Y \\ X \end{bmatrix} = \begin{bmatrix} 0 & -\alpha & 0 & 1 \\ -\mu x & 0 & \left(\frac{1-\mu}{2}\right) & 0 \\ 0 & \zeta^2 & 0 & -\alpha \\ -2(1+\mu)\alpha^2 + \zeta^2 & 0 & -\mu\alpha & 0 \end{bmatrix} \begin{bmatrix} U \\ V \\ Y \\ X \end{bmatrix}. \tag{4}$$

Let $\begin{bmatrix} U & V & Y & X \end{bmatrix}^T$ is denoted by $[S]$ the state vector, and then, equation (4) can be written as

$$\frac{d}{dy}[S] = [L][S]. \tag{5}$$

The vector-matrix differential equation is integrated to provide

$$[S] = \exp[y \cdot L] S(0). \tag{6}$$

The determinant's characteristic equation related to the matrix $[L_{ij}]$ can now be transcribed as

$$\left[\eta^2 + \left(\alpha^2 - \zeta^2\right)\right]\left[\eta^2 + \left(\alpha^2 - \frac{1-\mu}{2}\zeta^2\right)\right] = 0, \tag{7}$$

and the roots of this characteristic equation are

$$\eta = \pm i\delta_1, \pm i\delta_2, \tag{8}$$

in which

$$\delta_1 = \sqrt{\alpha^2 - \zeta^2}; \qquad \delta_2 = \sqrt{\alpha^2 - \frac{1-\mu}{2}\zeta^2}. \tag{9}$$

Every square matrix, according to the Cayley–Hamilton theorem, satisfies its characteristic equation. As a result, the exponential matrix is written as

$$\exp[yA] = a_0 I + a_1 A + a_2 A^2 + a_3 A^3. \tag{10}$$

Then, as per the characteristics of the eigenvalue of any square matrix, if the matrix A is substituted by its own eigenvalues, the equation must be satisfied:

$$\exp[y\eta] = a_0 + a_1\eta + a_2\eta^2 + a_3\eta^3. \tag{11}$$

Now, the roots obtained in equation (8) can be substituted in equation (11), and by resolving the simultaneous system of equation, the values of a_0, a_1, a_2, and a_3 can be found:

$$a_0 = 2\frac{\left(\delta_2^2 \cos y\delta_1 - \delta_1^2 \cos y\delta_2\right)}{(1+\mu)\zeta^2}, \quad a_1 = 2\frac{\left(\delta_2^2(\sin y\delta_1/\delta_1) - \delta_1^2(\sin y\delta_2/\delta_2)\right)}{(1+\mu)\zeta^2}, \quad a_2 = 2\frac{(\cos y\delta_1 - \cos y\delta_2)}{(1+\mu)\zeta^2}, \quad a_3 = 2\frac{((\sin y\delta_1/\delta_1) - (\sin y\delta_2/\delta_2))}{(1+\mu)\zeta^2}. \tag{12}$$

The transfer matrix $[L_{ij}]$ is produced by substituting these values in equation (10). We get the following equation from equation (6):

$$\begin{bmatrix} U \\ V \\ Y \\ X \end{bmatrix} = \begin{bmatrix} L_{UU} & L_{UV} & L_{UY} & L_{UX} \\ L_{VU} & L_{VV} & L_{VY} & L_{VX} \\ L_{YU} & L_{YV} & L_{YY} & L_{YX} \\ L_{XU} & L_{XV} & L_{XY} & L_{XX} \end{bmatrix} \begin{bmatrix} U_0 \\ V_0 \\ Y_0 \\ X_0 \end{bmatrix}. \tag{13}$$

The expressions for the values of constants from L_{UU} to L_{XX} are given as follows:

$$\begin{aligned}
L_{UU} &= L_{XX} = \frac{\left(-2\alpha^2 + \zeta^2\right)}{\zeta^2}\cos y\delta_1 + \frac{2\alpha^2}{\zeta^2}\cos y\delta_2, \\
L_{UV} &= L_{YX} = \frac{2\alpha\left(\alpha^2 - \zeta^2\right)}{\zeta^2\delta_1}\sin y\delta_1 - \frac{\alpha\left(2\alpha^2 - \zeta^2\right)}{\zeta^2\delta_2}\sin y\delta_2, \\
L_{UY} &= L_{VX} = -\frac{\alpha}{\zeta^2}\cos y\delta_1 + \frac{\alpha}{\zeta^2}\cos y\delta_2, \\
L_{UX} &= -\frac{\left(\alpha^2 - \zeta^2\right)}{\zeta^2\delta_1}\sin y\delta_1 + \frac{\alpha^2}{\zeta^2\delta_2}\sin y\delta_2, \\
L_{VU} &= L_{XY} = \frac{\alpha\left(2\alpha^2 - \zeta^2\right)}{\zeta^2\delta_1}\sin y\delta_1 - \frac{\alpha\left[2\alpha^2 - (1-\nu)\zeta^2\right]}{\zeta^2\delta_2}\sin y\delta_2, \\
L_{VV} &= L_{YY} = \frac{2\alpha^2}{\zeta^2}\cos y\delta_1 - \frac{\left(2\alpha^2 - \zeta^2\right)}{\zeta^2}\cos y\delta_2, \\
L_{VY} &= \frac{\alpha^2}{\zeta^2\delta_1}\sin y\delta_1 - \frac{\left(2\alpha^2 - (1-\nu)\zeta^2\right)}{2\zeta^2\delta_2}\sin y\delta_2, \\
L_{YU} &= L_{XV} = \frac{2\alpha\left(2\alpha^2 - \zeta^2\right)}{\zeta^2}\cos y\delta_1 - \frac{2\alpha\left(2\alpha^2 - \zeta^2\right)}{\zeta^2}\cos y\delta_2, \\
L_{YV} &= \frac{-4\alpha^2\left(\alpha^2 - \zeta^2\right)}{\zeta^2\delta_1}\sin y\delta_1 + \frac{\left(2\alpha^2 - \zeta^2\right)^2}{\zeta^2\delta_2}\sin y\delta_2, \\
L_{XU} &= \frac{\left(2\alpha^2 - \zeta^2\right)^2}{\zeta^2\delta_1}\sin y\delta_1 - \frac{2\alpha^2\left[2\alpha^2 - (1-\nu)\zeta^2\right]}{\zeta^2\delta_2}\sin y\delta_2.
\end{aligned} \tag{14}$$

3. Application to the Problem of Dynamic Analysis

We consider an elastic body that is being loaded from opposite directions (antisymmetric loading) while being constrained by two parallel planes for plane stress conditions. Because of the antisymmetric loading, we will choose $y = 0$ serving as the plane of reference:

$$U_0 = Y_0 = 0, \tag{15}$$

$y = \pm h$ on the plane,

$$Y = \pm p(x,t) \text{ with } X = 0. \tag{16}$$

We obtain the following equations by deleting the components involving U_0 and Y_0 in equation (13) and meeting the boundary constraints:

$$\begin{aligned}
Y(x,h,t) &= L_{YV}V_0 + L_{YX}X_0 = p(x,t), \\
X(x,h,t) &= L_{XV}V_0 + L_{XX}X_0 = 0.
\end{aligned} \tag{17}$$

We add an auxiliary function $F(x,t)$ to the equation so that

$$\begin{aligned}
L_{XV}F &= -X_0, \\
L_{XX}F &= V_0.
\end{aligned} \tag{18}$$

The first part of equation (17) leads to the differential equation for natural frequencies, whereas the second of equation (17) is equally satisfied:

$$L_{YV}L_{XX}F + L_{YX}L_{XV}F = p(x,t). \tag{19}$$

When the values of the operators are substituted, the exact partial differential equation is found as follows:

$$\left[\frac{\left(2\alpha^2-\zeta^2\right)^2}{\zeta^2\gamma_2}\cos h\gamma_1 \sin h\gamma_2 - \frac{4\alpha^2\left(\alpha^2-\zeta^2\right)}{\zeta^2\gamma_1}\sin h\gamma_1 \cos h\gamma_2\right]F = 0. \tag{20}$$

In equation (20), we expanded the trigonometric terms while keeping terms up to h^3; hence, a fourth-order differential equation is obtained. Furthermore, sixth-, eight-, and tenth-order differential equations can also be obtained by using trigonometric expansion of the terms in the equation and keeping the expressions to the desired order:

$$\left[\frac{2(1+\mu)}{3}h^3\alpha^4 - \frac{2}{3}(2+\mu)h^3\alpha^2\zeta^2 + \frac{7-\mu}{12}h^3\zeta^4 + h\zeta^2\right]F = 0. \tag{21}$$

In the expanded form, this will be

$$\left[\frac{2(1+\mu)}{3}h^3\frac{\partial^4}{\partial x^4} - \frac{2(2+\mu)\varrho}{3G}h^3\frac{\partial^4}{\partial x^2\partial t^2} + \frac{7-\mu}{12}h^3\left(\frac{\varrho}{G}\right)^2\frac{\partial^4}{\partial t^4} + \frac{h\varrho}{G}\frac{\partial^2}{\partial t^2}\right]F = 0. \tag{22}$$

To satisfy governing differential equation (19) and the beam's boundary conditions, the auxiliary function F is chosen. The necessary initial functions are provided by equation (18):

$$F_1 = A\sin\frac{n\pi x}{L}\cos\omega t. \tag{23}$$

In order to solve various problems and determine stresses and displacements, these functions were also engaged in Das and Setlur [32] and Patel et al. [44]:

$$\left[\frac{2(1+\mu)h^3}{3}\frac{\partial^4}{\partial x^4}\left(A\sin\frac{n\pi x}{L}\cos\omega t\right) - \frac{2}{3}(2+\mu)h^3A\frac{\partial^2}{\partial x^2}\sin\frac{\pi x}{L}\frac{\rho}{G}\frac{\partial^2}{\partial t^2}\cos\omega t + \frac{(7-\mu)h^3}{12}\frac{\rho^2}{G^2}\frac{d^4}{dt^4} \times A\sin\frac{\pi x}{L}\cos\omega t + \frac{h\rho}{G}\frac{\partial^2}{\partial t^2}A\sin\frac{\pi x}{L}\cos\omega t\right] = 0, \tag{24}$$

$$\left[\frac{2(1+\mu)h^3A}{3}\cos\omega t \times \frac{\pi^4}{L^4}\sin\left(\frac{\pi x}{L}\right) - \frac{2}{3}(2+\mu)h^3A\left(-\frac{\pi^2}{L^2}\right)\left(\sin\frac{\pi x}{L}\right)\frac{\rho}{G}\times\left(-\omega^2\cdot\cos\omega t\right) + \frac{(7-\mu)h^3\rho^2\times A\omega^4}{12G^2}\sin\frac{\pi x}{L}\cos\omega t - \frac{h\rho A\omega^2}{G}\sin\frac{\pi x}{L}\cos\omega t\right] = 0, \tag{25}$$

$$\left[\frac{2(1+\mu)h^3A}{3}\frac{\pi^4}{L^4}\sin\left(\frac{\pi x}{L}\right)\cos\omega t - \frac{2}{3}(2+\mu)h^3A\left(\frac{\pi^2}{L^2}\right)\left(\frac{\rho}{G}\omega^2\right)\left(\sin\frac{\pi x}{L}\cos\omega t\right) + \frac{(7-\mu)h^3\rho^2\times A\omega^4}{12G^2}\sin\frac{\pi x}{L}\cos\omega t - \frac{h\rho A\omega^2}{G}\sin\frac{\pi x}{L}\cos\omega t\right] = 0, \tag{26}$$

$$\left[\left\{\frac{(7-\mu)h^3\rho A}{12G^2}\right\}\omega^4 - \left\{\frac{2(2+\mu)h^3A\pi^2\rho}{3L^2G} - \frac{\rho hA}{G}\right\}\omega^2 + \left\{\frac{2(1+\mu)h^3A\pi^4}{3L^4}\right\}\right]\sin\frac{\pi x}{L}\cos\omega t = 0, \tag{27}$$

$$\left[\left\{\frac{(7-\mu)h^3\rho}{12G^2}\right\}\omega^4 - \left\{\frac{2(2+\mu)h^3\pi^2\rho}{3L^2G} - \frac{\rho h}{G}\right\}\omega^2 + \left\{\frac{2(1+\mu)h^3\pi^4}{3L^4}\right\}\right]\sin\frac{\pi x}{L}\cos\omega t = 0. \tag{28}$$

Solving this system, the natural frequency can be found.

4. Dynamic Analysis of an Isotropic Homogeneous Beam

Let us consider an isotropic homogeneous steel beam, the dimensions of the beam are chosen as follows:

Depth of beam (2h) = 800 mm and length of beam (L) = 4000 mm

We consider the following material characteristics:

For steel,

Elasticity modulus $E = 200000$ MPa

0.3 is the Poisson's ratio (μ)

The simply supported beam's boundary conditions are given as $u = 0, v = 0$ at $x = 0$ and $v = 0$ at $x = L$.

The auxiliary function is chosen to precisely satisfy the boundary criteria. On the upper surface of the beam, a load of 25 N/mm is applied uniformly.

Equation (23) yields the value of the auxiliary function F as

$$F_1 = A \sin \frac{\pi x}{L} \cos \omega t \quad \text{for } n = 1. \tag{29}$$

Equation (18) is used to obtain initial functions and with the help of equation (29), the deflection values and stresses for various depths of beam section are then obtained.

4.1. Poisson's Ratio. Poisson's ratio is a material property that describes how a material deforms in response to an applied load. It relates the strain in the direction perpendicular to the applied load to the strain in the direction of the load. Poisson's ratio is typically expressed as a dimensionless number. In many structural and mechanical systems, the natural frequency can be influenced by the material properties of the structure, including Poisson's ratio. When Poisson's ratio changes, it can affect the stiffness and mass distribution of the structure, which, in turn, can influence its natural frequency.

Table 1 presents Poisson's ratio (μ) values for various materials, including structural steel, limestone, and concrete. Poisson's ratio is an important material property affecting the response of materials to applied loads. Natural frequencies of beams made from these materials were calculated using equation (24), incorporating Poisson's ratio values from Table 1 as parameters.

The analysis reveals dependency between the natural frequency of the beams and Poisson's ratio. As Poisson's ratio increases, the natural frequency of the beams also increases, indicating a direct relationship. The impact of Poisson's ratio on natural frequency becomes more pronounced when considering a higher number of mode shapes or higher-frequency modes. This observation aligns with the phenomenon where complex and localized mode shapes are more sensitive to material properties. These findings have practical implications for structural engineering and design, highlighting the importance of considering how changes in material properties, such as Poisson's ratio, affect the dynamic behaviour of structures. This awareness is especially crucial when dealing with complex mode shapes or analysing structures for specific performance criteria.

Table 1: Poisson's ratio values for various materials.

Materials	Structural steel	Limestone	Concrete
Poisson's ratio (μ)	0.3	0.22	0.18
Modulus of elasticity (E)	200000 MPa	37845 MPa	30000 MPa

4.2. FEM Analysis. The 3 D modelling of the beam is carried out in ANSYS 2019 R2 Design Modeler. The SOLID186 element is used to model the beam. There are 20 nodes that make up this element, and each one has three degrees of freedom (translational x, y, and z directions). The beam comprises 25603 elements and 148536 nodes. Structural steel is taken as the material with Poisson's ratio of 0.3; various material characteristics, such as density (ρ) and Young's modulus (E), are assigned from engineering data sources in ANSYS. Material is considered homogeneous and isotropic for plane stress; the thickness is taken as 100 mm. For meshing, adaptive sizing is used along with an element size of 50 mm. Resolution is kept at 7 with fast transition, and smoothing is kept at medium. Maximum refinement loops are 2, and MAPDL-elapsed time is 9 seconds. The beam is designed for simply supported boundary conditions, and on the upper surface of the beam, an evenly distributed load of 25 N/mm is applied. Working out the problem with the help of the SOLVE command, the results in tabulated form can be obtained. The analysis approves the validation of the results. Figures 1–8 show the meshing of the beam, normal stresses for the beam, shear stresses for the beam, total deformations for the beam, directional deformations for the beam X axis, directional deformations for the beam Y axis, natural frequency referring to mode shape 1, and natural frequency referring to mode shape 25 obtained by ANSYS 2019 R2 Design Modeler.

5. Results and Discussion

Variation of shear stresses, normal stresses, total deformation, and natural frequency for isotropic homogeneous beams are shown in Figures 9–13.

Solving equation (28), along with equation (13), a beam element can be analysed along with all the parameters such as normal stresses and shear stresses. Figure 9 and Figure 10 show numerical examples. The problem parameters are $L = 4000$ mm, $2h = 800$ m, $\rho = 7850$ kg/m^3, $E = 200000$ MPa, and $\mu = 0.3$; in Figure 2, the shear stress curve is plotted using the relation obtained from (13). This figure shows the gradual increment in shear stress along the depth until it reaches the beam midpoint, and then, it decreases along the depth. The results obtained from MIFs and FEM are represented with different colours and are comparable. The results obtained through MIFs have a maximum deviation of

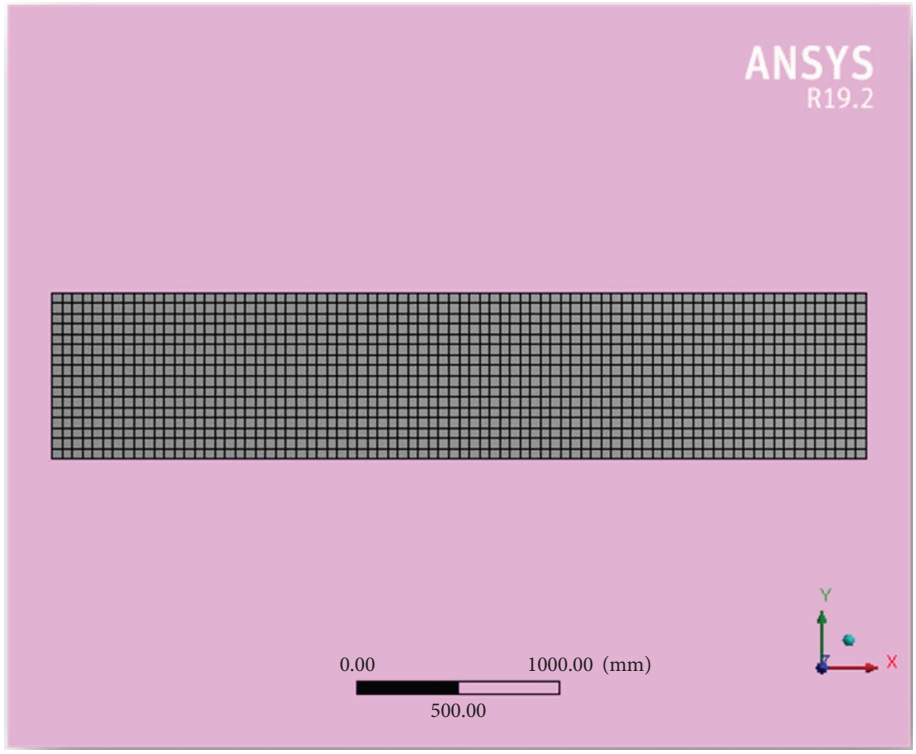

Figure 1: Meshing for the beam.

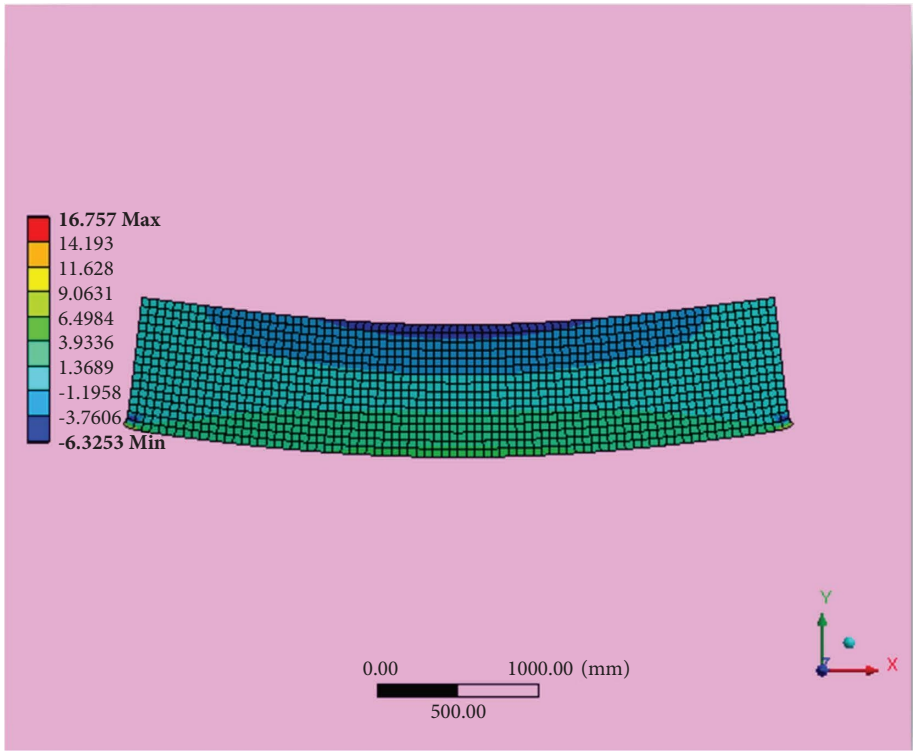

Figure 2: Normal stresses for the beam.

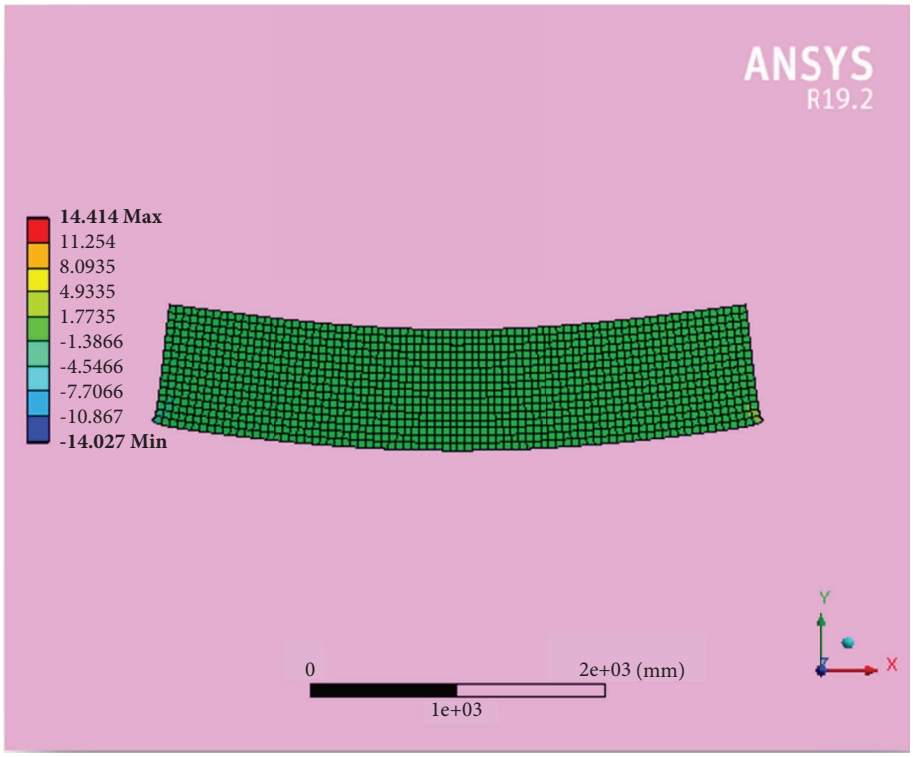

Figure 3: Shear stresses for the beam.

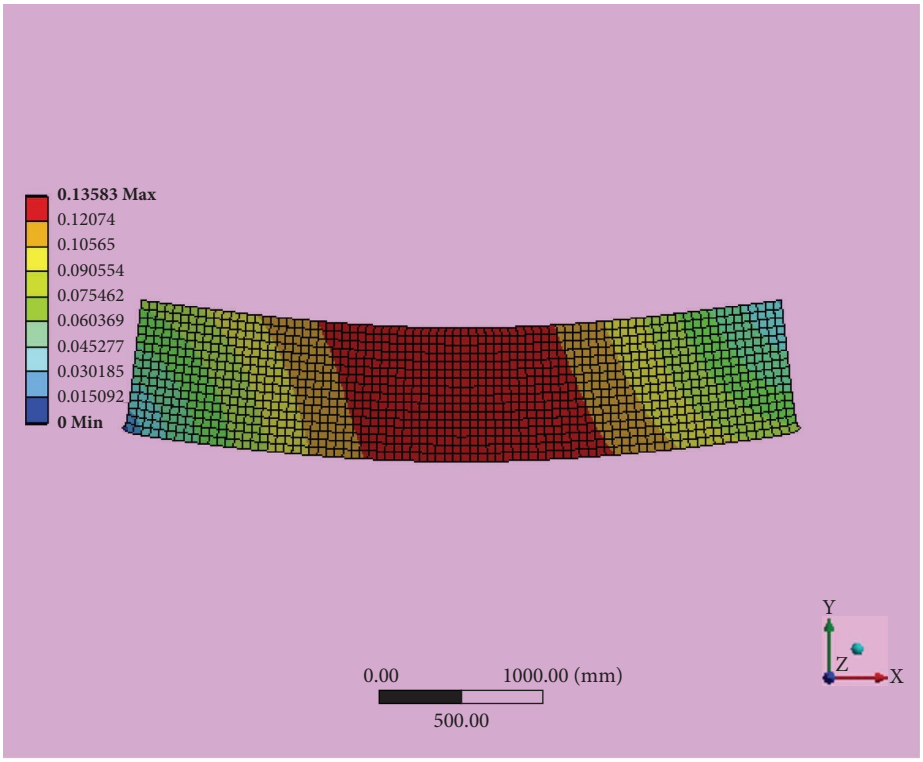

Figure 4: Total deformations for the beam.

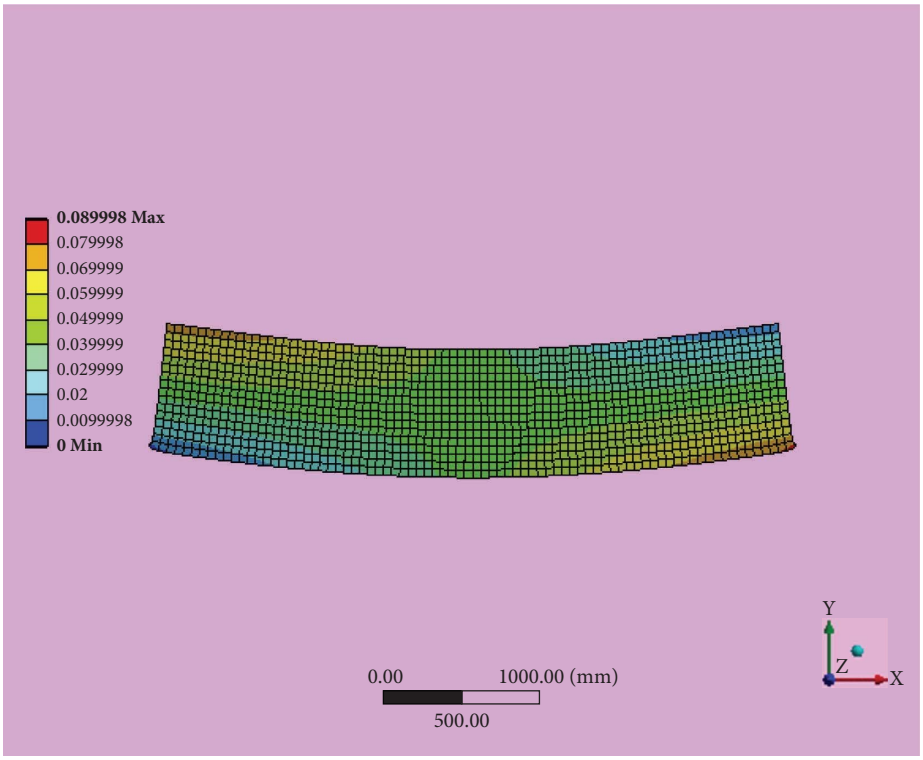

Figure 5: Directional deformations for the beam X axis.

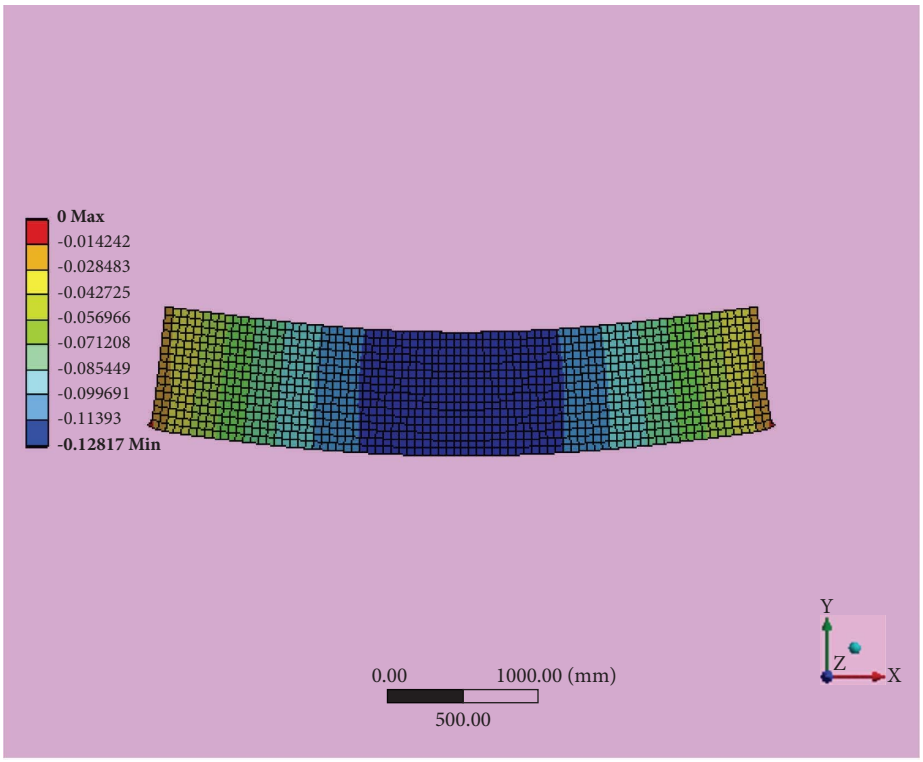

Figure 6: Directional deformations for the beam Y axis.

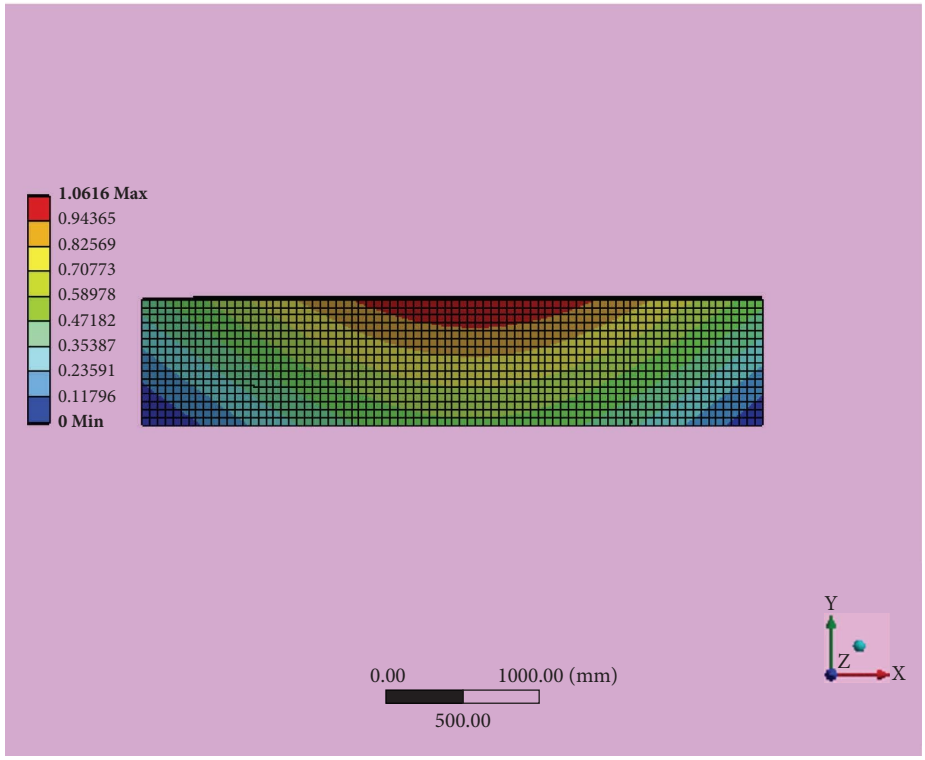

Figure 7: Natural frequency pertains to mode shape 1.

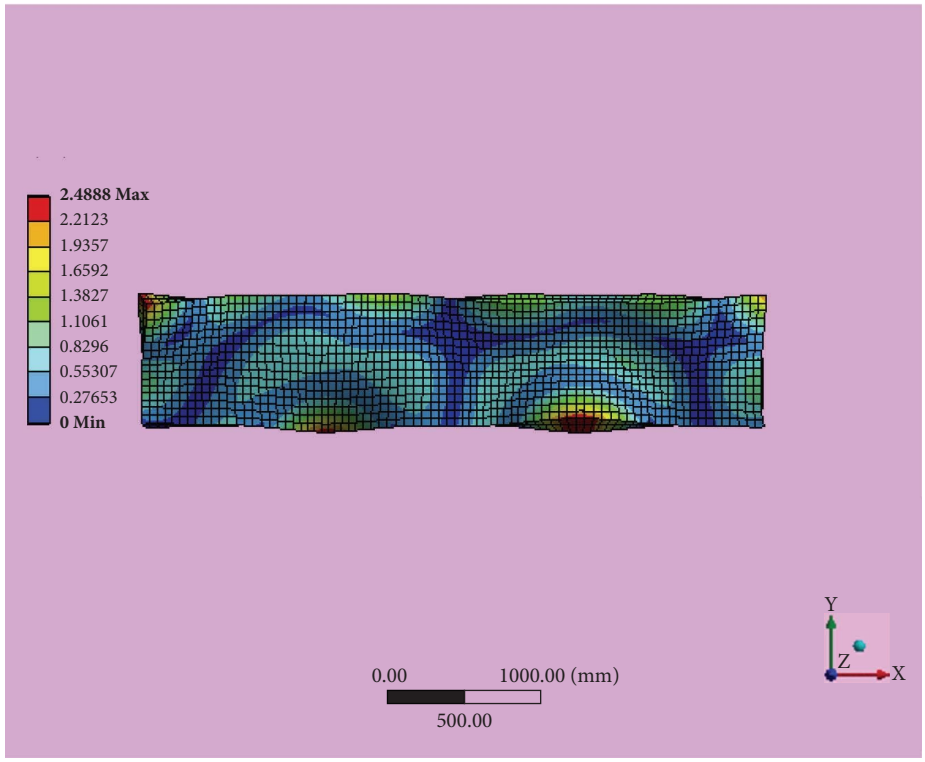

Figure 8: Natural frequency pertains to mode shape 25.

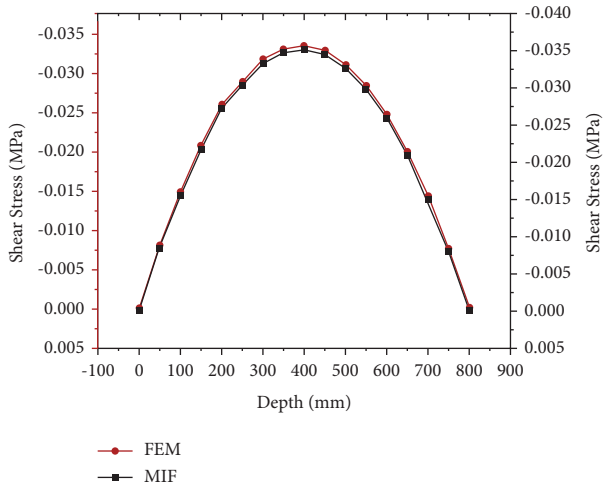

Figure 9: Comparison of MIFs and FEM for shear stresses (MPa).

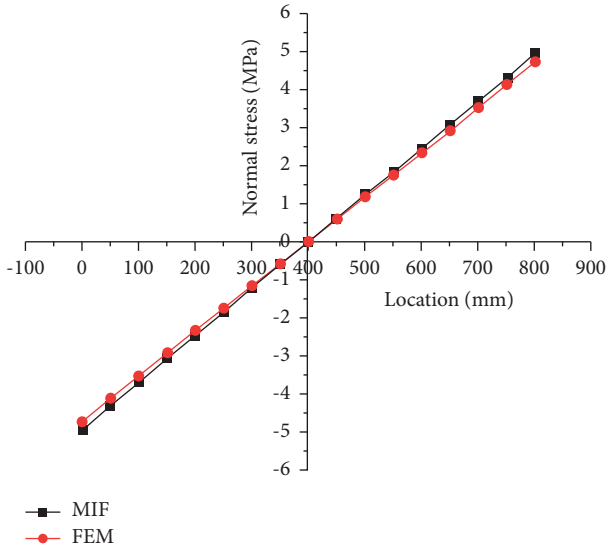

Figure 10: Comparison of MIFs and FEM for normal stress (MPa).

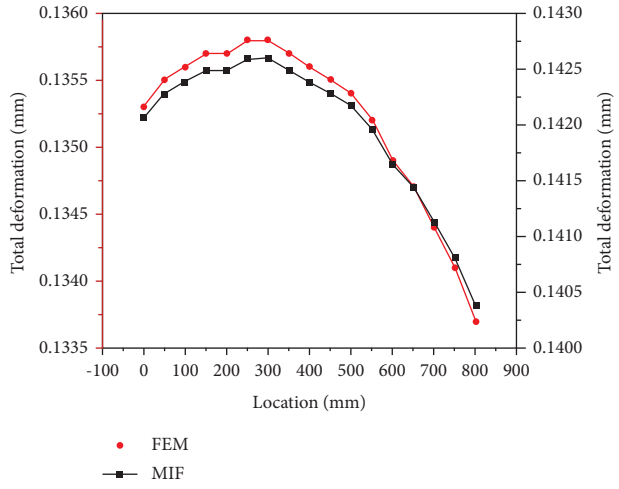

Figure 11: Comparison of MIFs and FEM for total deformation v (mm).

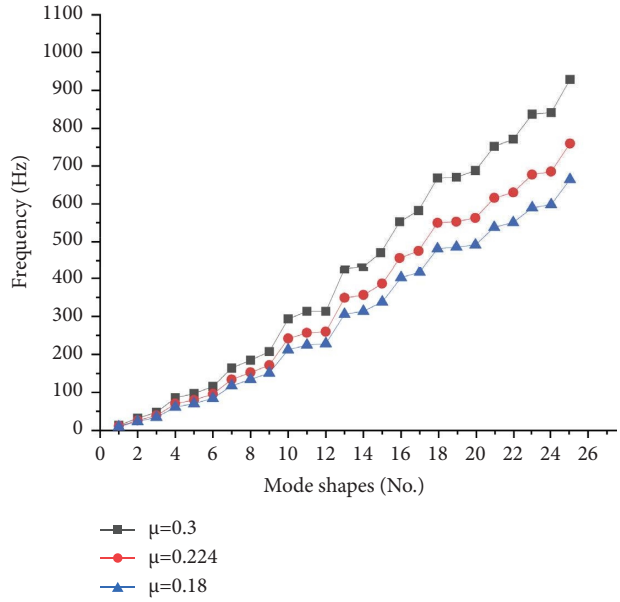

Figure 12: Variation of the beam's natural frequency for different values of μ.

0.17% and show the same patterns as those obtained through FEM.

In Figure 10, the normal stress curve is plotted using the relation obtained from equation (13). It clearly shows that the stress is maximum at the beam top and bottom; it decreases towards the middepth of the beam. The results obtained from MIFs and FEM are represented with different colours and are comparable. The results obtained through MIFs have a maximum deviation of 0.48% and show the same patterns as those obtained through FEM.

In Table 2, a detailed comparison of results of normal stresses calculated from classical theories such as Euler–Bernoulli beam theory, Timoshenko beam theory, and Rayleigh beam theory with MIF is given.

In Table 3, a detailed comparison of results of shear stresses calculated from classical theories such as Euler–Bernoulli beam theory, Timoshenko beam theory, and Rayleigh beam theory with MIF is given.

In Figure 11, the total deformation curve is plotted using the relation obtained from (13). This figure clearly shows the gradual increment in total deformation along the depth until it reaches a depth of 300 mm, and then, it decreases along the depth. The results obtained from MIFs and FEM are represented with different colours and are comparable. The results obtained through MIFs have a maximum deviation of 0.43% and show the same patterns as those obtained through FEM.

In Table 4, a detailed comparison of results of deflections calculated from classical theories such as Euler–Bernoulli beam theory, Timoshenko beam theory, and Rayleigh beam theory with MIF is given.

Figure 12 visually illustrates the relationship between Poisson's ratio and natural frequency, providing a clear

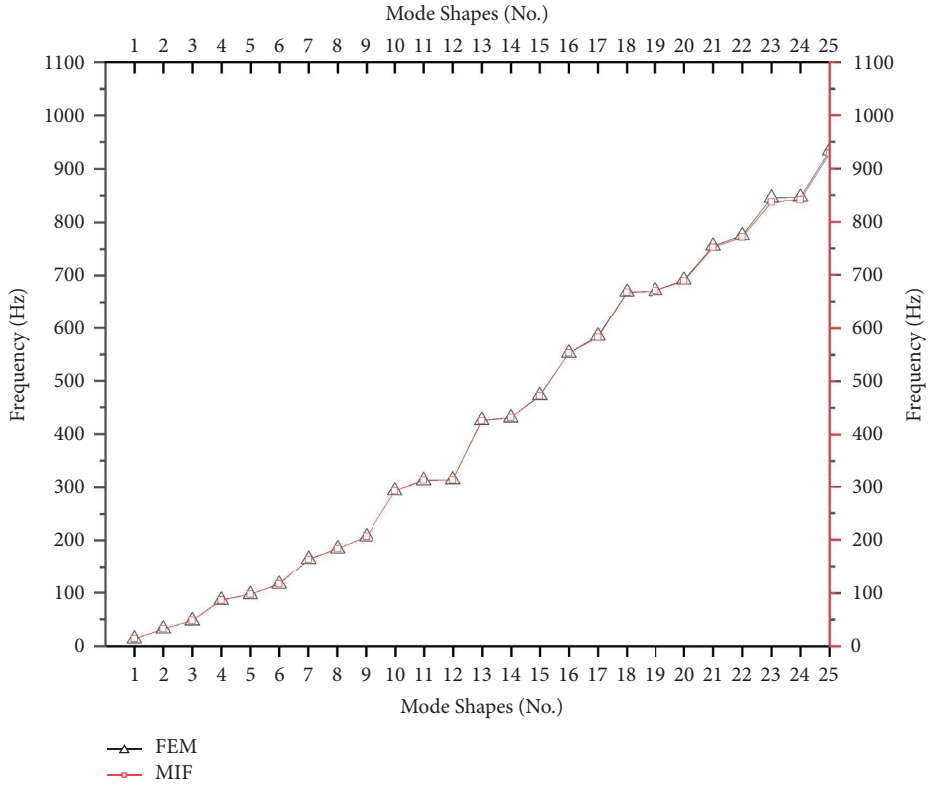

Figure 13: Natural frequency (Hz) results from MIFs and FEM.

Table 2: Comparison of normal stresses at different locations of simply supported beams subjected to uniformly distributed loads for different beam theories ($\mu = 0.3$).

Theories	Normal stresses at different locations								
	0	100	200	300	400	500	600	700	800
Euler–Bernoulli beam theory	−5.370624	−3.993948	−2.645622	−1.316574	−0.006804	1.330182	2.634282	3.990546	5.353614
Timoshenko beam theory	−5.271168	−3.919986	−2.596629	−1.292193	−0.006678	1.305549	2.585499	3.916647	5.254473
Rayleigh beam theory	−5.171712	−3.846024	−2.547636	−1.267812	−0.006552	1.280916	2.536716	3.842748	5.155332
MIF 8^{th} order	−5.072256	−3.772062	−2.498643	−1.243431	−0.006426	1.256283	2.487933	3.768849	5.056191
MIF 10^{th} order	−4.972800	−3.698100	−2.449650	−1.219050	−0.006300	1.231650	2.439150	3.694950	4.957050

representation of how changes in Poisson's ratio affect the natural frequency of the beams. To strengthen the research, we consider discussing the underlying mechanisms behind the dependence of natural frequency on Poisson's ratio, along with drawing conclusions from these findings and discussing their relevance to structural design and material selection.

It is important to clarify that the parametric study was conducted by varying the values of the modulus of elasticity in accordance with the materials listed in Table 1. This approach was adopted to ensure that the analysis accurately reflects the material-specific characteristics of the beams under consideration.

The entire parametric study is closely related to, and based on, the equation derived from the method of initial functions. This equation served as the foundational framework for the analysis, allowing for the systematic exploration of how changes in the modulus of elasticity and Poisson's ratio as specified for each material in Table 1 impact the natural frequencies of the beams.

To strengthen the argument and provide transparency in the study methodology, the values of modulus of elasticity corresponding to the materials listed in Table 1 have been included in the same table. This inclusion serves to explicitly link the variations in modulus of elasticity to the materials used in the analysis. By adjusting the modulus of elasticity based on the specific material properties listed in Table 1 and applying the equation from the method of initial functions, we aimed to capture the real-world behaviour of the beams more accurately. As a result, the parametric study accounts for the inherent material-dependent variations, contributing to a more comprehensive and realistic analysis of the natural frequencies of the beams.

Table 3: Comparison of shear stresses at different locations of simply supported beams subjected to uniformly distributed loads for different beam theories ($\mu = 0.3$).

Theories	Shear stress at different locations								
	0	100	200	300	400	500	600	700	800
Euler–Bernoulli beam theory	$-8.00E-05$	$-1.61E-02$	$-2.82E-02$	$-3.44E-02$	$-3.63E-02$	$-3.37E-02$	$-2.68E-02$	$-1.55E-02$	$-8.29E-05$
Timoshenko beam theory	$-7.85E-05$	$-1.58E-02$	$-2.76E-02$	$-3.38E-02$	$-3.56E-02$	$-3.30E-02$	$-2.63E-02$	$-1.52E-02$	$-8.14E-05$
Rayleigh beam theory	$-7.71E-05$	$-1.55E-02$	$-2.71E-02$	$-3.31E-02$	$-3.49E-02$	$-3.24E-02$	$-2.58E-02$	$-1.49E-02$	$-7.99E-05$
MIF 8^{th} order	$-7.56E-05$	$-1.52E-02$	$-2.66E-02$	$-3.25E-02$	$-3.43E-02$	$-3.18E-02$	$-2.53E-02$	$-1.46E-02$	$-7.83E-05$
MIF 10^{th} order	$-7.41E-05$	−0.0149	−0.02607	−0.03186	−0.0336	−0.03117	−0.0248	−0.01434	$-7.68E-05$

Table 4: Comparison of deflections at different locations of simply supported beams subjected to uniformly distributed loads for different beam theories ($\mu = 0.3$).

Theories	Total deformation at different locations															
	0	50	100	150	200	250	300	350	400	450	500	550	600	650	700	750
Euler–Bernoulli beam theory	0.153	0.154	0.154	0.154	0.154	0.154	0.154	0.154	0.154	0.154	0.154	0.153	0.153	0.153	0.152	0.152
Timoshenko beam theory	0.151	0.151	0.151	0.151	0.151	0.151	0.151	0.151	0.151	0.151	0.151	0.15	0.15	0.15	0.15	0.149
Rayleigh beam theory	0.148	0.148	0.148	0.148	0.148	0.148	0.148	0.148	0.148	0.148	0.148	0.148	0.147	0.147	0.147	0.146
MIF 8^{th} order	0.145	0.145	0.145	0.145	0.145	0.145	0.145	0.145	0.145	0.145	0.145	0.145	0.144	0.144	0.144	0.144
MIF 10^{th} order	0.142	0.142	0.142	0.142	0.142	0.143	0.143	0.142	0.142	0.142	0.142	0.142	0.142	0.141	0.141	0.141

Table 5: Values of natural frequency by 4^{th}, 6^{th}, 8^{th}, and 10^{th} order MIF theories.

Serial no.	No. of mode shapes	4^{th} order MIF	6^{th} order MIF	8^{th} order MIF	10^{th} order MIF
1	1	13.516	13.584	13.614	13.625
2	2	31.898	32.057	32.038	32.155
3	3	47.227	47.463	47.381	47.608
4	4	85.105	85.530	85.586	85.791
5	5	95.970	96.450	96.144	96.744
6	6	114.973	115.548	115.211	115.900
7	7	162.599	163.412	163.668	163.910
8	8	183.143	184.059	183.617	184.620
9	9	205.622	206.650	205.915	207.280
10	10	290.954	292.408	292.232	293.300
11	11	310.645	312.198	311.077	313.150
12	12	310.724	312.278	312.639	313.230
13	13	421.421	423.529	423.572	424.820
14	14	427.284	429.421	428.556	430.730
15	15	467.371	469.708	470.207	471.140
16	16	548.447	551.189	549.857	552.870
17	17	577.592	580.480	581.836	582.250
18	18	663.122	666.438	666.053	668.470
19	19	665.007	668.332	667.177	670.370
20	20	682.635	686.048	687.038	688.140
21	21	745.895	749.624	750.628	751.910
22	22	765.100	768.925	770.657	771.270
23	23	830.254	834.406	840.656	836.950
24	24	834.599	838.772	842.357	841.330
25	25	921.360	925.966	928.763	928.790

This approach ensures that the research accounts for the influence of material properties, including Poisson's ratio and modulus of elasticity, on the natural frequencies and strengthens the validity and relevance of the findings to practical engineering scenarios.

The initial functions can be determined with the help of equations (17) and (18), and after determining the values of X_0 and V_0, the stresses and displacements are determined. By solving the system of equations (24)–(28), the natural frequency can also be determined. In Figure 13, the natural frequency with respect to different mode shapes is calculated through the relation obtained in (24). This figure shows the closeness of results of natural frequencies obtained from two different approaches. These results are in complete agreement and are represented with different colours. The results obtained through MIFs have a minimum deviation of −0.16% and a maximum deviation of 0.94% and follow the same patterns as those obtained through FEM.

Table 5 shows the values of natural frequencies obtained from different order MIF theories. These orders of MIF theories are determined by keeping the different powers of h in the trigonometric expansion in equation (20). However, the precision of the theory increases with the order of MIF theory; this is more applicable in structures with higher dimensions, such as deep beams. This method is particularly of interest where ordinary theories, such as Euler–Bernoulli beam theory, Timoshenko beam theory, and Rayleigh beam theory, fail to give accurate results. Another advantage of using this theory is that it does not depend on any assumption; it is entirely dependent on symbolic mathematics.

Its fundamental structure is according to elasticity theory. It also uses the condition of plane stress with the amalgamation of the equations used in the above theory and condition. With symbolic mathematics, we reached the above-mentioned results.

6. Conclusions

This research work is concluded as follows:

(1) As symbolic mathematics progresses, the competences of MIFs inscribed in the space of different mathematical transforms are substantially improved. Continued advancements in symbolic mathematics and their integration with MIFs can lead to even more powerful tools for dynamic analysis.

(2) Dynamic behaviour of the beam is investigated using the MIFs. The advantage of MIF is that it does not require any assumptions about the location of the neutral axis; also, the analysis is not restricted up to a certain extreme elastic limit of a material.

(3) When compared with classical theories such as Euler–Bernoulli beam theory, Timoshenko beam theory, and Rayleigh beam theory, MIF produces conceptually precise and exact values of results.

(4) An exact solution to the problem is obtained. The higher-order analysis tends to give a precise result which is verified by the fourth-, sixth-, eight-, and tenth-order MIF theories.

(5) When compared with natural frequency results, it is found that there is a maximum deviation of 0.94% and a minimum deviation of −0.16%.

(6) Poisson's ratio (μ) considerably affects natural frequency, and the value of natural frequency drops as Poisson's ratio decreases.

(7) Variation in normal stresses is almost negligible. Variation of the displacement values (v) is nearly linear across the depth, and its value is greater in the case of MIFs. In both theories, the variation in results of shear stress across the depth is almost nonexistent.

(8) Future work holds the promise of expanding these findings into diverse materials, structural applications, and analytical methods, thereby contributing to more efficient and precise dynamic analysis in engineering and other fields.

Nomenclature

u: Deflection in x direction
v: Deflection in y direction
E: Elasticity modulus
G: Shear modulus
A: Area of cross section
L: Length of the beam
2h: Depth of the beam
σ_x: Bending stress
τ_{yx}: Shear stress
ρ: Density
σ_y: Normal stress
μ: Poisson's ratio
η: Eigenvalue of square matrix
ω: Natural frequency of harmonic vibration
FEM: Finite element method
MIFs: Method of initial functions
DQM: Differential quadrature method
CFM: Complementary function method
FGCP: Functionally graded composite panels
FSDT: First-order shear deformation shell theory
CNTRC: Carbon nanotube-reinforced composite plates.

Data Availability

The data used to support the findings of the study are included within the article.

Conflicts of Interest

The authors declare that they have no conflicts of interest.

Authors' Contributions

Jitendra Namdeo was responsible for conceptualization, writing of the original draft, and investigation. S. K. Dubey was responsible for reviewing and editing and supervision. Lobzang Dorji was responsible for designing the methodology, proofreading, and editing.

Acknowledgments

The first author would like to thank the Maulana Azad National Institute of Technology, Bhopal (India), for supporting and providing resources to complete this research work.

References

[1] J. Thomas and B. A. H. Abbas, "Finite element model for dynamic analysis of Timoshenko beam," *Journal of Sound and Vibration*, vol. 41, no. 3, 1975.

[2] Y. W. Kim and S. C. Cha, "Finite element formulation and analysis of Timoshenko beam excited by transversely fluctuating supports due to a real seismic wave," *Nuclear Engineering and Technology*, vol. 50, no. 6, pp. 971–980, 2018.

[3] M. P. Singh and M. Ghafory-Ashtiany, "Modal time history analysis OF NON-classically damped structures for seismic motions," *Earthquake Engineering and Structural Dynamics*, vol. 14, no. 1, pp. 133–146, 1986.

[4] D. M. Seyedi, P. Gehl, J. Douglas, L. Davenne, N. Mezher, and S. Ghavamian, "Development of seismic fragility surfaces for reinforced concrete buildings by means of nonlinear time-history analysis," *Earthquake Engineering and Structural Dynamics*, vol. 39, no. 1, pp. 91–108, 2010.

[5] A. K. Chopra, "Elastic response spectrum: a historical note," *Earthquake Engineering and Structural Dynamics*, vol. 36, no. 1, pp. 3–12, 2007.

[6] A. K. Gupta, B. Raton, L. New, and Y. Washington, *Response Spectrum Method in Seismic Analysis and Design of Structures*, CRC Press, Boca Raton, FL, USA, 2017.

[7] G. Solari and P. de Gaetano, "Dynamic response of structures to thunderstorm outflows: response spectrum technique vs time-domain analysis," *Engineering Structures*, vol. 176, pp. 188–207, 2018.

[8] M. Baghani, H. Mazaheri, and H. Salarieh, "Analysis of large amplitude free vibrations of clamped tapered beams on a nonlinear elastic foundation," *Applied Mathematical Modelling*, vol. 38, no. 3, pp. 1176–1186, 2014.

[9] H. Babaei, Y. Kiani, and M. R. Eslami, "Large amplitude free vibrations of FGM beams on nonlinear elastic foundation in thermal field based on neutral/mid-plane formulations," *Iranian Journal of Science and Technology- Transactions of Mechanical Engineering*, vol. 45, no. 3, pp. 611–630, 2021.

[10] R. Vatankhah, A. Najafi, H. Salarieh, and A. Alasty, "Exact boundary controllability of vibrating non-classical Euler-Bernoulli micro-scale beams," *Journal of Mathematical Analysis and Applications*, vol. 418, no. 2, pp. 985–997, 2014.

[11] H. Salarieh and M. Ghorashi, "Free vibration of Timoshenko beam with finite mass rigid tip load and flexural-torsional coupling," *International Journal of Mechanical Sciences*, vol. 48, no. 7, pp. 763–779, 2006.

[12] J. W. Jaworski and E. H. Dowell, "Free vibration of a cantilevered beam with multiple steps: comparison of several theoretical methods with experiment," *Journal of Sound and Vibration*, vol. 312, no. 4–5, pp. 713–725, 2008.

[13] A. E. Alshorbagy, M. A. Eltaher, and F. F. Mahmoud, "Free vibration characteristics of a functionally graded beam by finite element method," *Applied Mathematical Modelling*, vol. 35, no. 1, pp. 412–425, 2011.

[14] A. G. Shenas, P. Malekzadeh, and S. Ziaee, "Vibration of triangular functionally graded carbon nanotubes reinforced composite plates with elastically restrained edges in thermal environment," *Iranian Journal of Science and Technology-Transactions of Mechanical Engineering*, vol. 43, no. S1, pp. 653–678, 2019.

[15] P. Malekzadeh and Y. Heydarpour, "Free vibration analysis of rotating functionally graded cylindrical shells in thermal environment," *Composite Structures*, vol. 94, no. 9, pp. 2971–2981, 2012.

[16] P. Malekzadeh, A. R. Fiouz, and M. Sobhrouyan, "Three-dimensional free vibration of functionally graded truncated conical shells subjected to thermal environment," *International Journal of Pressure Vessels and Piping*, vol. 89, pp. 210–221, 2012.

[17] S. Pouresmaeeli, S. A. Fazelzadeh, and E. Ghavanloo, "Exact solution for nonlocal vibration of double-orthotropic nanoplates embedded in elastic medium," *Composites Part B: Engineering*, vol. 43, no. 8, pp. 3384–3390, 2012.

[18] S. Pouresmaeeli and S. A. Fazelzadeh, "Frequency analysis of doubly curved functionally graded carbon nanotube-reinforced composite panels," *Acta Mechanica*, vol. 227, no. 10, pp. 2765–2794, 2016.

[19] M. Mirzaei and Y. Kiani, "Free vibration of functionally graded carbon nanotube reinforced composite cylindrical panels," *Composite Structures*, vol. 142, pp. 45–56, 2016.

[20] P. Malekzadeh and A. R. Zarei, "Free vibration of quadrilateral laminated plates with carbon nanotube reinforced composite layers," *Thin-Walled Structures*, vol. 82, pp. 221–232, 2014.

[21] Y. Kiani, "Free vibration of FG-CNT reinforced composite skew plates," *Aerospace Science and Technology*, vol. 58, pp. 178–188, 2016.

[22] Y. Kiani, "Free vibration of functionally graded carbon nanotube reinforced composite plates integrated with piezoelectric layers," *Computers and Mathematics with Applications*, vol. 72, no. 9, pp. 2433–2449, 2016.

[23] Y. Kiani, R. Dimitri, and F. Tornabene, "Free vibration study of composite conical panels reinforced with FG-CNTs," *Engineering Structures*, vol. 172, pp. 472–482, 2018.

[24] S. Yildirim, "An efficient method for the plane vibration analysis of composite sandwich beam with an orthotropic core," *Cumhuriyet Science Journal*, vol. 41, no. 2, pp. 521–526, 2020a.

[25] S. Yildirim, "Free vibration analysis of sandwich beams with functionally-graded-cores by complementary functions method," *AIAA Journal*, vol. 58, no. 12, pp. 5431–5439, 2020b.

[26] X. Liu, Y. Li, Y. Lin, and J. R. Banerjee, "Spectral dynamic stiffness theory for free vibration analysis of plate structures stiffened by beams with arbitrary cross-sections," *Thin-Walled Structures*, vol. 160, Article ID 107391, 2021.

[27] S. Yildirim, "Free vibration of axially or transversely graded beams using finite-element and artificial intelligence," *Alexandria Engineering Journal*, vol. 61, no. 3, pp. 2220–2229, 2022.

[28] A. R. Noori and S. Yildirim, "Effect of the finite element modeling techniques on the dynamic analysis of beams," *Adıyaman Üniversitesi Mühendislik Bilimleri Dergisi*, vol. 9, no. 18, pp. 581–590, 2022.

[29] M. A. Al-Zahrani, S. A. Asiri, K. I. Ahmed, and M. A. Eltaher, "Free vibration analysis of 2D functionally graded strip beam using finite element method," *Journal of Applied and Computational Mechanics*, vol. 8, no. 4, pp. 2383–4536, 2022.

[30] S. Marzavan and V. Nastasescu, "Free vibration analysis of a functionally graded plate by finite element method," *Ain Shams Engineering Journal*, vol. 14, no. 8, Article ID 102024, 2023.

[31] M. Tan, D. Guo, Q. Yang, L. Yang, and D. Luo, "In-plane and out-of-plane free vibration analysis of thin-walled box beams based on one-dimensional higher-order beam theory," *Mechanics of Advanced Materials and Structures*, pp. 1–15, 2023.

[32] Y. C. Das and P.-A. V. Setlur, "Method of initial functions in two-dimensional elastodynamic problems," *Journal of Applied Mechanics*, vol. 37, 1970.

[33] A. V. Matrosov, "An exact analytical solution for a free-supported micropolar rectangle by the method of initial functions," *Zeitschrift Fur Angewandte Mathematik Und Physik*, vol. 73, no. 2, p. 74, 2022.

[34] K. T. Sundara, R. Iyengar, and S. K. Pandya, "Analysis of orthotropic rectangular thick plates," *Fibre Science and Technology*, vol. 18, 1983.

[35] K. T. Sundara Raja Iyengar and P. V. Raman, "Free vibration of rectangular plates of arbitrary thickness," *Journal of Sound and Vibration*, vol. 54, no. 2, pp. 229–236, 1977.

[36] K. Sundara Raja Iyengar, P. Raman, and P. V. Raman, "Free vibration of rectangular plates of arbitrary thickness with one or more edges clamped," *Journal of Sound and Vibration*, vol. 71, no. 4, pp. 463–472, 1980.

[37] K. Celep, "On the elastodynamic theory of thick circular plates," *Journal of Applied Mathematics and Mechanics*, vol. 323, no. 80, 1980.

[38] Z. Celep, "On the axially symmetric vibration of thick circular plates," *Ingenieur-Archiv*, vol. 47, no. 6, pp. 411–420, 1978.

[39] D. P. Goloskokov and A. V. Matrosov, "Approximate analytical approach in analyzing an orthotropic rectangular plate with a crack," *Materials Physics and Mechanics*, vol. 36, no. 1, pp. 137–141, 2018.

[40] M. D. Kovalenko, I. V. Men'shova, and T. D. Shulyakovskaya, "Expansions in Fadle-Papkovich functions: examples of

solutions in a half-strip," *Mechanics of Solids*, vol. 48, no. 5, pp. 584–602, 2013.

[41] M. D. Kovalenko and T. D. Shulyakovskaya, "Expansions in Fadle-Papkovich functions in a strip. Theory foundations," *Mechanics of Solids*, vol. 46, no. 5, pp. 721–738, 2011.

[42] R. Patel, S. K. Dubey, and K. K. Pathak, "Analysis of RC brick filled composite beams using MIF," *Procedia Engineering*, vol. 51, pp. 30–34, 2013.

[43] L. A. Petrosyan and P. Zhabko, "Sankt-Peterburgskiĭ gosudarstvennyĭ universitet," in *Proceedings of the International Conference "Stability and Control Processes" in Memory of V.I. Zubov (SCP): SCP-BDO-2015*, Institute of Electrical and Electronics Engineers. Russia North-West Section, Institute of Electrical and Electronics Engineers, and International Workshop, Saint-Petersburg, Russia, October, 2015.

[44] R. Patel, S. K. Dubey, and K. K. Pathak, "Effect of elastic properties on the behaviour of beams," *International Journal of Structural Engineering*, vol. 5, no. 1, pp. 43–53, 2014.

[45] R. Patel, S. K. Dubey, and K. K. Pathak, "Analysis of infilled beams using method of initial functions and comparison with FEM," *Engineering Science and Technology, an International Journal*, vol. 17, no. 3, pp. 158–164, 2014.

[46] P. Asutkar, S. B. Shinde, and R. Patel, "Study on the behaviour of rubber aggregates concrete beams using analytical approach," *Engineering Science and Technology, an International Journal*, vol. 20, no. 1, pp. 151–159, 2017.

[47] A. V. Matrosov, M. D. Kovalenko, I. V. Menshova, and A. P. Kerzhaev, "Method of initial functions and integral Fourier transform in some problems of the theory of elasticity," *Zeitschrift Fur Angewandte Mathematik Und Physik*, vol. 71, no. 1, p. 24, 2020.

[48] R. Patel, S. K. Dubey, and K. K. Pathak, *Proceedings of the Indian Structural Steel Conference 2020 (Vol. 1)*, Springer, Berlin, Germany, 2023.

[49] K. T. Sundara Raja Iyengar and P. V. Raman, "Free vibration of rectangular beams of arbitrary depth," *Acta Mechanica*, vol. 32, no. 4, pp. 249–259, 1979.